Gene Expression Analysis of Preinvasive and Invasive Cervical Squamous Cell Carcinomas Identifies *HOXC10* as a Key Mediator of Invasion

Yali Zhai,[1] Rork Kuick,[3] Bin Nan,[4] Ichiro Ota,[2] Stephen J. Weiss,[2,3] Cornelia L. Trimble,[5] Eric R. Fearon,[1,2,3] and Kathleen R. Cho[1,2,3]

Departments of [1]Pathology and [2]Internal Medicine, and [3]The Comprehensive Cancer Center, The University of Michigan Medical School; [4]Department of Biostatistics, University of Michigan School of Public Health, Ann Arbor, Michigan; and [5]Department of Gynecology and Obstetrics, The Johns Hopkins University School of Medicine, Baltimore, Maryland

Abstract

If left untreated, a subset of high-grade squamous intraepithelial lesions (HSIL) of the cervix will progress to invasive squamous cell carcinomas (SCC). To identify genes whose differential expression is linked to cervical cancer progression, we compared gene expression in microdissected squamous epithelial samples from 10 normal cervices, 7 HSILs, and 21 SCCs using high-density oligonucleotide microarrays. We identified 171 distinct genes at least 1.5-fold up-regulated (and $P < 0.001$) in the SCCs relative to HSILs and normal cervix samples. Differential expression of a subset of these genes was confirmed by quantitative reverse transcription-PCR and immunohistochemical staining of cervical tissue samples. One of the genes up-regulated during progression, *HOXC10*, was selected for functional studies aimed at assessing its role in mediating invasive behavior of neoplastic squamous epithelial cells. Elevated HOXC10 expression was associated with increased invasiveness of human papillomavirus–immortalized keratinocytes and cervical cancer–derived cell lines in both *in vitro* and *in vivo* assays. Cervical cancer cells with high endogenous levels of HOXC10 were less invasive after short hairpin RNA–mediated knockdown of HOXC10 expression. Our findings support a key role for the HOXC10 homeobox protein in cervical cancer progression. Other genes with differential expression in invasive SCC versus HSIL may contribute to tumor progression or may be useful as markers for cancer diagnosis or progression risk. [Cancer Res 2007;67(21):10163–72]

Introduction

Cervical cancer is the third leading cause of cancer deaths in women worldwide, with increased mortality in less developed regions compared with the industrialized world. For example, cervical cancer–associated mortality in East Africa is nearly 14-fold higher than in North America (1). Cervical cancer incidence and mortality have decreased dramatically over the last several decades in many countries, largely as a consequence of widely implemented Pap smear screening programs that allow detection and removal of cervical cancer precursors referred to as squamous intraepithelial lesions (SIL). The highest grade squamous cervical cancer precursor lesions, referred to as high-grade SILs (HSIL), are very prevalent in the United States, with an estimated age-adjusted incidence of 31 per 100,000 women (2). Although it is difficult to determine the natural history of HSILs, it has been estimated that as few as 12% of high-grade preinvasive lesions will progress to carcinoma if left untreated (3). In a recent prospective observational study, 28% of colposcopically visible residual HSILs regressed within 15 weeks of diagnostic biopsy (4). Because morphologic assessment alone does not allow distinction of the HSILs likely to progress from those that will regress or simply persist, essentially all HSILs are currently treated by surgical excision or with ablative therapies. Identification of molecular markers defining the subset of HSILs at high risk for progression could clearly affect management of preinvasive cervical lesions.

Over the last 30 years, substantial progress has been made in understanding the molecular basis of cervical cancer. Infection with certain (high-risk) types of human papillomaviruses (HPV) is strongly associated with the development of both preinvasive and invasive cervical epithelial neoplasms (5). A few characteristic genetic alterations have been identified in invasive cervical carcinomas (6–8) but relatively little is known about the specific molecular alterations that allow preinvasive epithelial cells to acquire the ability to penetrate the basement membrane and invade the underlying stroma. Notably, the majority of HSILs have been shown to be clonal and aneuploid (9, 10), and the lesional cells in HSILs display many if not most of the same morphologic features as their frankly malignant counterparts.

To identify genes associated with the invasive properties of cervical carcinoma cells, we used high-density (Affymetrix U133A) oligonucleotide microarrays to generate comprehensive gene expression profiles of microdissected epithelial samples from normal cervices, HSILs, and invasive squamous cell carcinomas (SCC) of the cervix. Comparison of gene expression in the preinvasive and invasive epithelial neoplasms identified a rather modest number of genes differentially up-regulated or down-regulated in SCCs relative to HSILs and normal cervical squamous epithelia. Our differential expression screen identified several genes that may prove useful as diagnostic or progression markers for cervical cancer; a subset of these genes encodes proteins that confer invasive properties to neoplastic cervical epithelial cells.

Materials and Methods

Cell lines and cell culture. Seven cervical carcinoma–derived cell lines, C-33A, C-4II, ME-180, CaSki, SiHa, HT-3, and HeLa, were obtained from the American Type Culture Collection. The HPV16-immortalized keratinocyte cell line 8217 was a gift from P. Hawley-Nelson (Department of Molecular Discovery, Centocor, Inc., Radnor, PA). The HPV18-immortalized

Note: Supplementary data for this article are available at Cancer Research Online (http://cancerres.aacrjournals.org/).

Requests for reprints: Kathleen R. Cho, Department of Pathology, University of Michigan Medical School, 1506 BSRB, 109 Zina Pitcher, Ann Arbor, MI 48109-2200. Phone: 734-764-1549; Fax: 734-647-7950; E-mail: kathcho@umich.edu.

doi:10.1158/0008-5472.CAN-07-2056

keratinocyte cell line 1811 and its NMU-transformed counterpart, NMU-T1, were a gift from J.K. McDougall (Fred Hutchinson Cancer Research Center, Seattle, WA; ref. 11). CIN612 [derived from grade 1 cervical intraepithelial neoplasia or CIN1 (also known as low-grade SIL or LSIL)] and the HPV18-immortalized cervical keratinocyte cell line 610, were a gift of K. De Geest (Rush Medical College, Chicago, IL; ref. 12). ME-180 and HT-3 cells were cultured in McCoy's 5A medium (Life Technologies, Inc.) with 10% fetal bovine serum (FBS, Life Technologies). CaSki cells were cultured in RPMI 1640/10% FBS. Keratinocyte-derived cells (NMU-T1, 1811, 8217, 610, and CIN612) were cultured in keratinocyte growth medium (Clonetics Corp.). All other cell lines were maintained in DMEM with 10% FBS.

Tissue samples and laser capture microdissection. A total of 21 frozen invasive SCCs of the cervix, 7 HSILs, and 10 normal cervix samples were analyzed with approval from the institutional review board (IRB) of the University of Michigan Medical School. Invasive SCC specimens were obtained from the University of Michigan and Johns Hopkins Hospitals and from a previous study conducted in Spain and Colombia (13). Frozen HSIL specimens were banked as part of an IRB-approved prospective clinical trial at the Johns Hopkins Hospital designed to estimate the spontaneous regression rate of HSIL over a 15-week observational period (4). The normal cervical tissues were harvested from hysterectomy specimens resected for benign disease. Slides were prepared for laser capture microdissection (LCM) following the manufacturer's protocol provided with the Arcturus HistoGene LCM Frozen Section Staining Kit. Neoplastic squamous epithelial cells from HSILs or invasive carcinomas were isolated using an Arcturus PixCell IIe LCM system with CapSure HS LCM Caps for each sample. A cervical tissue microarray was constructed from an independent set of samples selected from the Surgical Pathology archives at the University of Michigan. The tissue microarray block includes representative cores from 15 normal cervix, 20 LSIL, 21 HSIL, and 26 SCC samples.

HPV detection and typing. HPV detection and typing were done on each tissue sample using PCR amplification of HPV DNA, followed by direct sequencing. The GP5+/GP6+, L1C1/LlC2, and/or L1C2-M consensus primers were used for HPV DNA detection (14, 15). All HPV-negative samples were confirmed by a second PCR assay and adequate DNA quality was verified by successful amplification of *HPRT1* sequences from the same DNA samples (Supplementary Table S1). PCR products were purified with the GENECLEAN III Kit (MP Biomedicals) and directly sequenced. DNA sequences were compared with Genbank sequences using the BLAST Program at the National Center for Biotechnology Information (NCBI). In selected cases, HPV types were further confirmed by HPV E7 type–specific PCR using published primer sequences (16).

RNA isolation, amplification, and gene expression profiling. Total RNA from LCM-harvested lesional cells was extracted from each sample using the Arcturus PicoPure RNA isolation Kit (KIT0202). RNA quality was determined by detecting 28S/18S rRNA peaks with an Agilent Bioanalyzer 2100 (Agilent Technologies). Two rounds of T7-based RNA amplification were carried out with the Arcturus RiboAmp kit (KIT 0201) following the manufacturer's instructions. Total RNA from each cell line was extracted using standard procedures (TRIzol reagent, Invitrogen). Labeling of cRNA, hybridization, and scanning of the microarrays were done according to the manufacturer's protocols, as reported previously (17). High-density oligonucleotide microarrays [HG_U133A arrays (22,283 probe sets); Affymetrix] were used in this study.

Data processing and statistical analysis. Array hybridization, scanning, and image analysis were done according to the manufacturer's protocols (Affymetrix). Probe-set intensities were obtained and normalized as previously described, using publicly available software (17). Data were log-transformed using $Y = \log[\max(X + 50,0) + 50]$. Fold changes between groups were computed based on averages of the transformed data. Annotations indicating the gene represented by each probe set as of July 14, 2006, were obtained from the Affymetrix web site. The array data are available from the NCBI Gene Expression Omnibus[6] using series accession number GSE7803.

[6] http://www.ncbi.nlm.nih.gov/geo/

Quantitative reverse transcription-PCR. Quantitative reverse transcription-PCR (qRT-PCR) was used to validate differential expression of selected genes in RNA isolated from cell lines and cervical tissue specimens after LCM, but without RNA amplification. qRT-PCR was done with an ABI Prism 7700 Sequence Analyzer using SYBR green fluorescent protocol (PE Applied Biosystems). qRT-PCR reactions for target and internal control genes were done in separate tubes. The comparative threshold cycle (C_T) method was used to compare the level of mRNA expression of genes of interest to that of a control gene. Primer sequences for *HOXC10, HOXC6, APOC1, HPRT1* (internal control), and *GAPDH* (internal control) are indicated in Supplementary Table S1. Each reaction was set up in duplicate and two separate measurements were carried out.

Immunohistochemistry. Formalin-fixed, paraffin-embedded tissues were immunostained using standard techniques. Antigen retrieval was enhanced by microwaving the slides in citrate buffer (pH 6.0, Biogenex) for 10 min. Sections were incubated with rabbit polyclonal anti-ECT2 (1:500 dilution), anti-FOXM1 (1:300 dilution), or mouse monoclonal anti-RCF4 (1:300 dilution) antibody (Santa Cruz Biotechnology, Inc.) or anti-TK1 antibody (1:200 dilution, Novus Biologicals, Inc.) overnight at 4°C. Antigen-antibody complexes were detected with the avidin-biotin peroxidase method using 3,3′-diaminobenzidine as a chromogenic substrate (Vectastain ABC kit, Vector Laboratories). Sections were lightly counterstained with hematoxylin and examined by light microscopy.

***In situ* hybridization detection of *HOXC10* expression.** A cDNA fragment spanning *HOXC10* nucleotides 915 to 1,340 was subcloned into the pPST18 and pPST19 vectors (Roche Diagnostics GmbH) for generation of sense and antisense probes, respectively. Digoxigenin-labeled riboprobes were prepared with T7 RNA polymerase using the DIG RNA labeling kit (Roche Diagnostics). Details of our *in situ* hybridization protocol have been described previously (18). Hybridization signals were detected with nitroblue tetrazolium/5-bromo-4-chloro-3-indolylphosphate. Sections were counterstained with 0.1% nuclear fast red and examined by light microscopy.

Northern blot analysis. Total RNA was extracted from cultured cells using TRIzol reagent (Invitrogen). Ten micrograms of total RNA were separated on 1.2% formaldehyde-agarose gels and transferred to Zeta-Probe GT-membranes (Bio-Rad) by capillary action. Human *HOXC10* and *GAPDH* cDNA fragments were amplified by PCR using primer sequences indicated in Supplementary Table S1 and were labeled with [^{32}P]dCTP by random hexamer priming. Northern blot hybridization was carried out in RapidHyb Buffer (Invitrogen) according to the manufacturer's protocol. Signals were detected by exposure to BioMax-MS film (Kodak) at −80°C with an intensifying screen.

Expression vector construction and transfection. Full-length *HOXC10* cDNA (spanning nucleotides 99 to 1,127, Genbank accession no. NM_017409) was generated by RT-PCR using total RNA from HeLa cells. The PCR primers were designed to include a FLAG epitope tag at the HOXC10 COOH terminus. PCR products were subcloned into the retroviral vector pPGS-CMV-CITE-neo and the cDNA sequence of individual clones verified by automated DNA sequencing. Selected cell lines (610, 1811, and HeLa) were transduced with retroviral supernatant from amphotrophic Phoenix cells transfected with vector alone or vector with *HOXC10*. Stable polyclonal lines were generated by selection in G418 at a concentration of 0.2 to 1 mg/mL. After 1 week, the G418 concentration was reduced to 0.1 to 0.4 mg/mL, and expression of Flag-tagged HOXC10 protein was confirmed by Western blot analysis. Stably transduced cells were lysed in cold radioimmunoprecipitation assay lysis buffer containing proteinase inhibitors (complete proteinase inhibitors, Roche Applied Science). Whole-cell lysates were analyzed by Western blotting with anti-FLAG M2 antibody (Sigma) at 1:5,000. Expression of β-actin was used as a loading control and was detected with anti-actin polyclonal antibody (Sigma).

Short hairpin RNA–mediated knockdown of HOXC10 expression in ME180 cells. To obtain polyclonal ME180 cell lines stably expressing two independent *HOXC10*-specific short hairpin RNAs (shRNA) or control scrambled shRNA, cells were transduced with lentiviruses that drive expression of shRNA from the H1 promoter as well as green fluorescent protein from a CMV promoter. shRNA vectors were originally made in the

pSUPERIOR PURO plasmid (Oligoengine) by cloning annealed oligonucleotides into the *Bgl*II-*Hin*dIII–digested vector. Sequences of the *HOXC10*-specific and control oligonucleotides were designed using the Dharmacon *siDESIGN* center[7] and are shown in Supplementary Table S1. Subsequently, an *Xho*I-*Xma*I fragment comprising the H1 promoter and shRNA sequence was shuttled into the Lentilox 3.7 vector (19), in which the U6 promoter was replaced with a polylinker. Lentiviral vectors encoding shRNAs were cotransfected with packaging vectors into 293T cells as described (19). Supernatant was collected every 12 h and incubated with ME180 cells in the presence of 4 μg/mL polybrene (Sigma). After three rounds of infection, medium was replaced and cells were allowed to grow for 48 h. The efficiency of *HOXC10* knockdown was determined using quantitative RT-PCR.

Colony formation in soft agar. Soft agar assays of HeLa cell lines were done using standard techniques. Briefly, 5,000 cells were plated in DMEM with 17% FCS containing 0.3% soft agar on top of an underlayer containing 0.6% soft agar in six-well plates. Plates were fixed with glutaraldehyde and stained with methylene blue (Sigma) after 3 weeks. Colony number and size were determined with assistance of NIH ImageJ software.

Wound scratch migration assay. Cells were plated in six-well plates and grown to 80% to 90% confluence. Cell monolayers were scratched with a 1-mm-wide sterile plastic scraper and rinsed twice with PBS, then incubated in complete medium in the absence or presence of epidermal growth factor (EGF; 10 ng/mL). To determine the leading front of cell migration, images were taken at 0, 24, 48, and 72 h later, using a microscope equipped with a SPOT cooled color digital camera (Diagnostic Instruments).

Matrigel transmembrane invasion assay. Transwell chambers (Corning Costar) with inserts containing 8-μm pores were coated with 200 μL of 1:3 diluted Matrigel (BD Biosciences) in serum-free medium. Cells (2.5×10^5–5×10^5) were plated in the upper chamber of the transwells or six-well invasion chambers (BD Biosciences) and allowed to invade across the Matrigel-coated membrane for 24 to 48 h. Medium containing EGF (10 ng/mL) as a chemoattractant was added to the bottom well. After noninvading cells were removed from the top of each membrane with wet cotton swabs, invading cells attached to the bottom of the membrane were fixed and stained with Diff Quick Stain Kit (IMEB, Inc.) or 4′,6-diamidino-2-phenylindole (DAPI). The number of cells that penetrated the membrane was determined by counting the mean cell number of five randomly selected high power (×40) fields. Experiments were done in triplicate.

Chick embryo chorioallantoic membrane invasion assay. Fertilized eggs were purchased from a local poultry farm (Bilbie Aviaries). The embryos were incubated for 11 days at 37°C with 60% humidity. Preparation of CAMs has been described in detail in the published literature (20, 21). To grow tumor masses, 2.5×10^6 cells labeled with 0.05 μm fluoresbrite carboxylate microspheres (Polysciences) in 40 μL of HBSS were applied on the chorioallantoic membrane (CAM). After 3 to 6 days, the tumor masses and surrounding CAM were excised and fixed with 4% paraformaldehyde in PBS overnight at 4°C. Frozen sections were cut from the CAM tissues after immersion in 30% sucrose and mounted with Vectashield mounting medium with DAPI (Vector Laboratories), then visualized under a fluorescent microscope (Leica DMLB) and photographed with a SPOT cooled color digital camera (Diagnostic Instruments). Adjacent sections were also prepared and stained with H&E for light microscopic examination.

Results

Identification of genes differentially expressed in SCCs versus HSILs and normal cervical epithelia. To restrict our analysis to the appropriate epithelial cells present in each cervical tissue specimen, we used LCM to enrich samples for the desired epithelial cell populations. LCM was used to harvest cells from 7 HSILs, 21 invasive SCCs, and 10 samples of normal squamous cervical epithelia. The "captured" cell populations were largely free of contaminating stromal, endothelial, and inflammatory cells. Representative examples before and after LCM are shown in Supplementary Fig. S1. Total RNA was extracted from each microdissected sample. A typical yield was ~20 to 100 ng of RNA from 1,000 to 5,000 captured cells. The RNA samples were subsequently amplified using two rounds of T7-based *in vitro* transcription (IVT) to generate sufficient quantities of RNA for cRNA labeling and hybridization to the oligonucleotide microarrays. To determine whether the amplified cRNA from the samples accurately represent the relative abundance of mRNAs in the starting material, we compared the gene expression profile from 5 μg of RNA sample extracted from a primary cervical carcinoma (C-2T) undergoing a single round of IVT (as part of the standard preparation of labeled cRNA for hybridization to microarrays), to a 100 ng sample of RNA from the same specimen amplified with two rounds of IVT. Based on hybridization of labeled cRNAs to U133A oligonucleotide microarrays, the expression data from the standard (5 μg) and twice-amplified (100 ng) samples are highly correlated (Pearson's correlation coefficient, 0.87; Supplementary Fig. S2*A*). To assess effects of LCM on gene expression profiling, we compared gene expression from the 100 ng C-2T sample above, isolated from a tumor cell-rich region without LCM, and 30 ng of total RNA were isolated from C-2T by LCM, both using two rounds of IVT. For this comparison, Pearson's correlation coefficient was 0.90 (Supplementary Fig. S2*B*). Finally, to determine reproducibility of the linear amplification protocol, we compared gene expression in two RNA samples extracted from another primary cervical carcinoma (CS-87), again, both amplified by the T7-based protocol: 15 ng of total RNA from tumor cells were isolated by LCM, and 30 ng of total RNA from tumor cells were isolated by LCM. For this comparison, Pearson's correlation coefficient was 0.96 (Supplementary Fig. S2*C*). These results indicate that LCM coupled with two rounds of T7-based IVT allows accurate and reproducible determination of gene expression profiles from small samples, particularly when all samples are processed and analyzed in a similar manner.

Using LCM and two rounds of T7-based IVT, we generated comprehensive gene expression profiles from cervical SCCs, HSILs, and normal cervical squamous epithelium samples. Principal component analysis determined that the three types of specimens are separable based on their global gene expression profiles (Supplementary Fig. S3). Intermediate- and/or high-risk HPV types were identified in all of the carcinomas, 6 of 7 HSILs, and 1 (weakly positive for HPV18) of 10 normal cervix samples (Supplementary Table S2), indicating that differences in gene expression profiles are not related to the presence, absence, or type of HPV. Not surprisingly, when the first two principal components are plotted, gene expression in the HSILs falls roughly between that of the normal cervix and SCC samples. We compared gene expression between SCC (n = 21) versus HSIL (n = 7) and normal cervix (n = 10) using a one-way ANOVA, and selected probe sets that gave $P < 0.001$ for comparing both SCC versus HSIL and SCC versus normal cervix for which the SCC samples had mean expression 1.5-fold above or below the means of both other groups. This selected 297 probe sets (195 higher in SCC, 102 lower), of which we estimate that only 0.1 are expected to be false positives, based on a similar analysis of 1,000 data sets in which the sample labels were randomly permuted. Figure 1 shows a smaller subset of these genes, for which the fold change was larger than 2.5-fold. The entire data set and statistical analysis appears in Supplementary Table S3.

Validation of microarray data. We used qRT-PCR to validate differential expression of selected genes identified by the microarray

[7] http://www.dharmacon.com

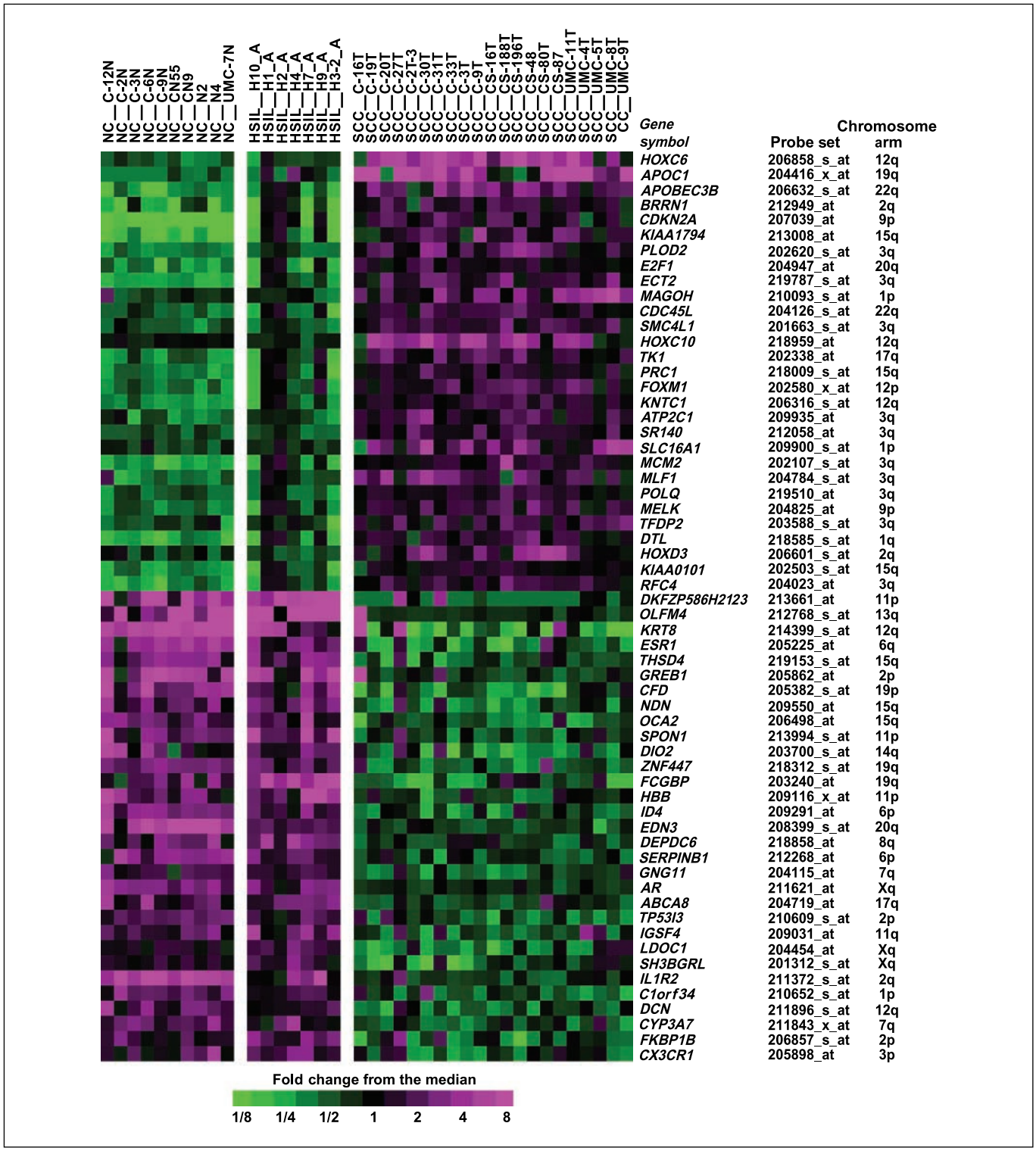

Figure 1. Gene expression signature of cervical SCCs. Differentially expressed genes were identified by asking that comparisons of SCCs to HSILs as well as SCCs compared with normal cervix samples both give $P < 0.001$ from a one-way ANOVA and show at least 2.5-fold difference in the means. This comparison yielded 29 genes with higher expression in SCCs and 31 genes with lower expression in SCCs relative to the other groups. Fold change from the median level in normal cervix samples and gene location with respect to chromosome arm are shown.

analysis. Validation studies were done using 32 of the 38 samples from which the gene expression profiles were generated. These included 19 SCCs, 5 HSILs, and 8 normal cervix samples with sufficient RNA available after LCM. Three up-regulated genes (*HOXC6, HOXC10*, and *APOC1*) were selected for qRT-PCR analysis and the data were highly correlated to the microarray data for all three genes, with expression differences between SCCs and HSILs for each gene readily apparent (Fig. 2*A*). We also selected a subset

of differentially expressed genes (*ECT2, FOXM1, RFC4*, and *TK1*) encoding proteins for which suitable antibodies were commercially available, and used immunohistochemical analysis to determine whether differential mRNA expression results in detectable differences in protein expression (Fig. 2*B*). Invasive carcinomas showed increased expression for each of these proteins relative to normal cervix and HSIL, based on immunohistochemical studies of individual tissue sections and a tissue microarray containing an independent set of normal and neoplastic cervical tissue samples.

HOXC10 is highly expressed in most cervical carcinomas and stimulates keratinocyte motility and invasion. We wished to determine whether our differential expression screen identified genes with a key contributing role in the invasive phenotype of cervical carcinoma cells and we selected *HOXC10* for further analysis. First, *in situ* hybridization was done to verify differential expression of *HOXC10* transcripts in normal cervical tissue, HSILs, and SCCs. As indicated in Fig. 3*A*, *HOXC10* transcripts localize to tumor cells, with strongest expression in invasive carcinomas, relatively weaker expression in HSILs, and virtual absence of *HOXC10* expression in squamous epithelium from normal cervix. We also used Northern blot analysis to examine *HOXC10* expression in a panel of cervical carcinoma-derived and HPV-immortalized keratinocyte cell lines (Fig. 3*B*). *HOXC10* expression was readily detectable in most of the cervical carcinoma–derived cell lines, but was virtually undetectable in CIN-derived 612 cells and HPV18-immortalized cervical keratinocytes (610).

To determine whether increased expression of HOXC10 can enhance invasiveness of squamous epithelial cells, cell lines expressing various levels of endogenous *HOXC10* were stably transfected with a FLAG-tagged full-length *HOXC10* cDNA (Fig. 4*A*). Cells lacking endogenous *HOXC10* transcripts (i.e., 610 cells) or expressing modest levels of endogenous *HOXC10* transcripts (i.e., 1811 and

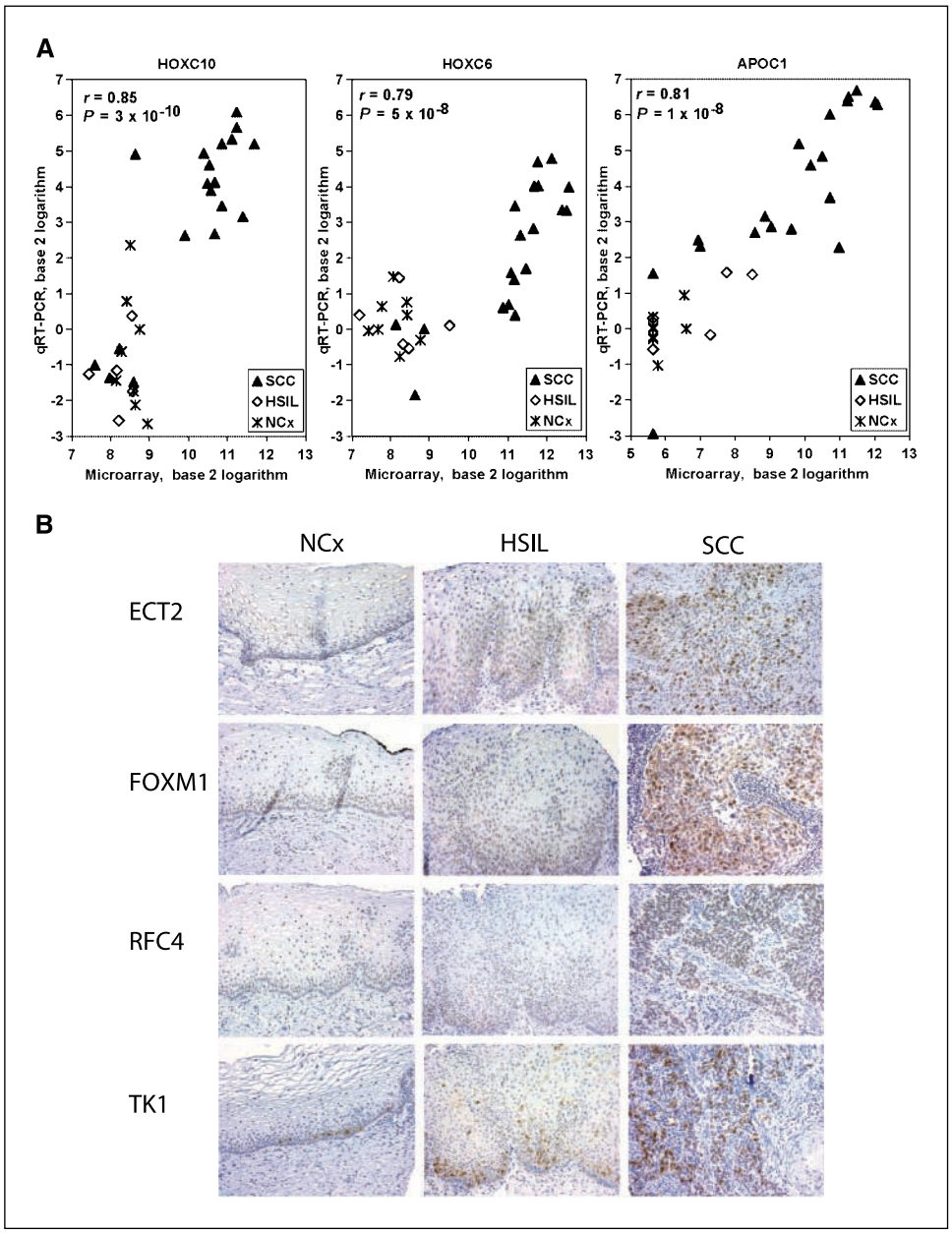

Figure 2. Validation of microarray data by qRT-PCR and immunohistochemistry. *A,* comparison of *HOXC10, HOXC6*, and *APOC1* gene expression from microarray and qRT-PCR analyses. RNA for qRT-PCR were extracted from SCC (n = 19), HSIL (n = 5), and normal cervix (n = 8) samples isolated by LCM. For each gene, the mean relative expression (normalized to *HPRT1*) based on qRT-PCR analysis is plotted against the expression measure obtained from the microarray analysis. The Pearson's correlation (r) and its significance (P) are given. *B,* immunohistochemical analysis of Ect2, FoxM1, Rfc4, and TK1 protein expression in representative normal cervix (*NCx*), HSIL, and SCC tissue samples. Tissue sections were immunostained with antibodies recognizing the indicated proteins. Original magnification, ×200.

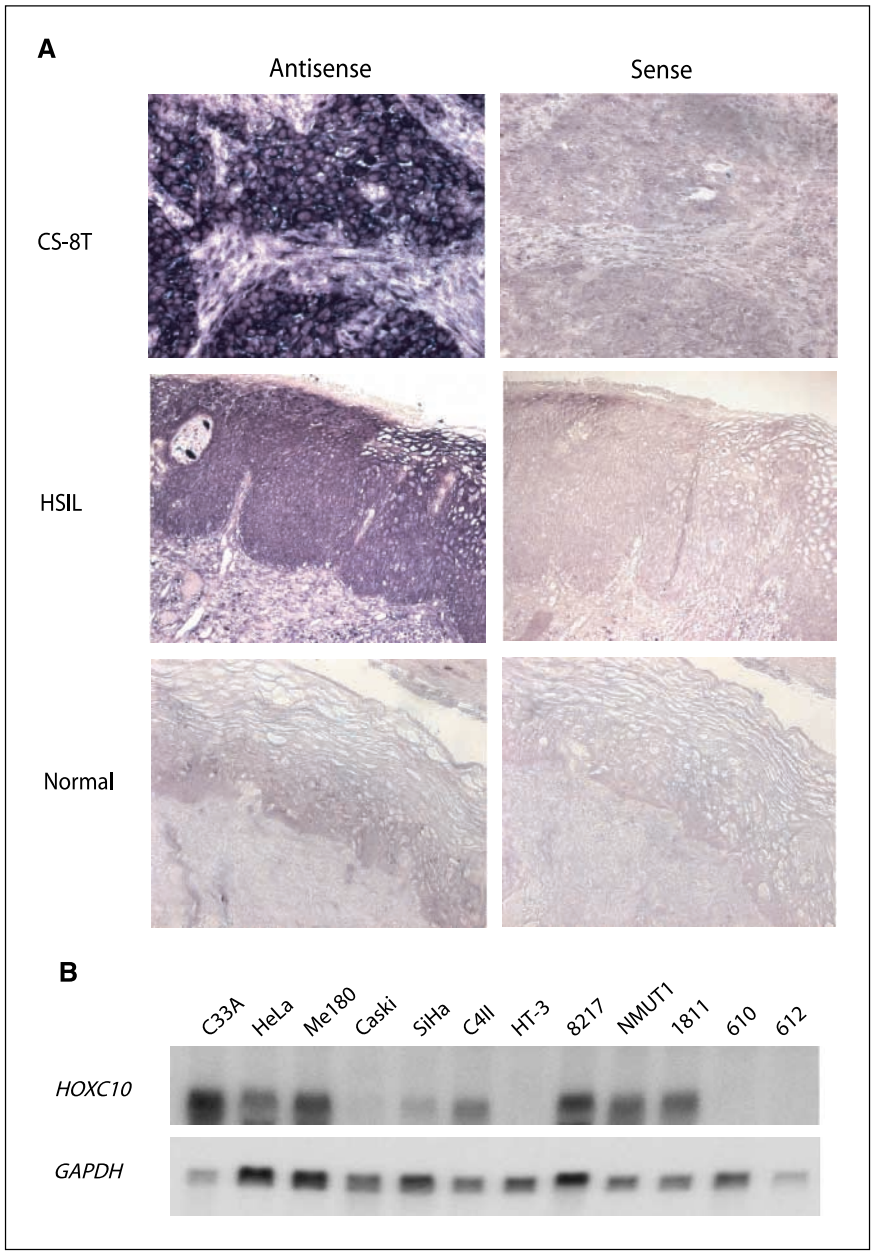

Figure 3. *HOXC10* expression in cervical tissue samples and cell lines. *A, in situ* hybridization was used to detect *HOXC10* transcripts in primary tissue samples. Sections from invasive SCCs, HSILs, and normal cervical tissues were hybridized with digoxigenin-labeled *HOXC10* antisense (*left panels*) and sense (*right panels*) riboprobes. Original magnification, ×400. *B,* Northern blot analysis of *HOXC10* mRNA in the indicated cell lines; expression of *GAPDH* was used as a loading control.

HeLa cells) were selected for these studies. First, a "wound scratch" assay was done to determine whether expression of HOXC10 regulated migration/motility of 1811- and/or 610 HPV–immortalized keratinocytes. Overexpression of HOXC10 enhanced migration compared with control cell lines transfected with vector alone, particularly when stimulated with EGF (data not shown). Effects of HOXC10 on invasion of 610, 1811, and HeLa cells was further assessed using Matrigel-coated transwell inserts. The 610 cells transduced with vector alone or with *HOXC10* showed no invasion through Matrigel (data not shown), whereas 1811 and HeLa cells ectopically expressing *HOXC10* showed increased invasion through Matrigel compared with control (Fig. 4*B*). Increased expression of HOXC10 in HeLa cells also resulted in increased colony number and size in soft agar assays (Fig. 4*C*). To determine whether HOXC10 can modulate the invasive properties of cervical epithelial cells in an *in vivo* assay that more closely mimics invasion of neoplastic epithelial cells through the basement membrane and into underlying cervical stroma, cells with and without exogenous HOXC10 expression were tested for invasion of the chick CAM. HeLa, 1811, and 610 cells stably transduced with *HOXC10* or vector alone were labeled with fluorescent microspheres and applied to the surface of the chick CAM. Cells lacking endogenous *HOXC10* (610-neo) failed to invade the CAM after 6-day incubation, but 610 cells expressing *HOXC10* invaded the CAM at the same time point (Fig. 5). Moreover, the CAM-invasive phenotype of cells with modest endogenous HOXC10 expression (1811-neo and HeLa-neo) was markedly enhanced by expression of exogenous HOXC10.

shRNA-mediated knockdown of HOXC10 reduces invasiveness of ME180 cervical carcinoma cells. Having shown that increased expression of HOXC10 increases invasiveness of HPV-immortalized keratinocytes and cervical carcinoma–derived cells, we wished to determine whether inhibition of HOXC10 expression

reduced invasiveness of cervical cancer cells. We used stable expression of shRNAs to inhibit HOXC10 expression in ME180 cervical cancer cells, which express high levels of endogenous *HOXC10* (Fig. 3*B*). Two independent shRNAs showed substantial reduction of HOXC10 expression compared with a scrambled sequence control shRNA (Fig. 6*A*). ME180 cells with reduced HOXC10 expression showed less invasiveness through Matrigel in the transwell invasion assay (Fig. 6*B* and *C*). Taken together, the findings support HOXC10 as an important mediator of invasion in the progression of HSIL to invasive carcinoma.

Discussion

Although a number of gene expression profiling studies of invasive cervical carcinomas have been reported (22–26), only a few have attempted to generate comprehensive gene expression profiles from preinvasive cervical squamous intraepithelial lesions (27, 28). This may be due, at least in part, to difficulty obtaining frozen samples of intraepithelial cervical lesions from which high-quality RNA can be extracted. The standard of clinical care usually mandates that cervical biopsies with suspected intraepithelial lesions be fixed in formalin, embedded in paraffin, and submitted in their entirety for diagnostic evaluation. In this study, we were able to analyze a rather unusual group of frozen HSIL samples collected as part of an IRB-approved clinical trial (4). The majority of HSILs occur in women of child-bearing age and ablative treatment using cone biopsy, electrocautery, laser, or cryotherapy causes significant morbidity and consumes considerable health care resources. Novel molecular markers aiding distinction

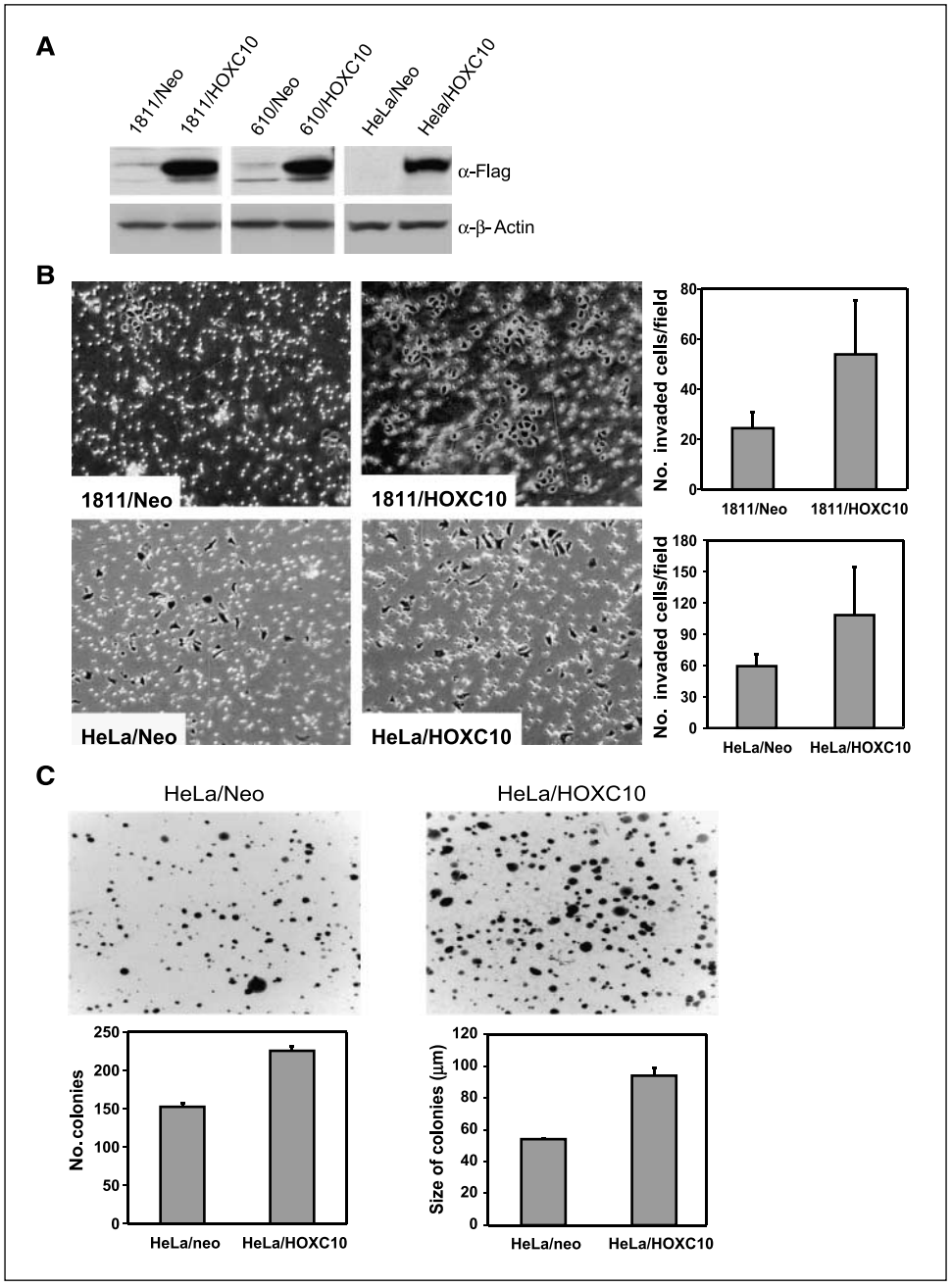

Figure 4. HOXC10 stimulates epithelial cell invasion and anchorage-independent growth. *A,* Western blot analysis of lysates from indicated cell lines after stable transduction with replication-deficient retroviruses expressing full-length *HOXC10* or control retrovirus. Flag-tagged exogenous HOXC10 was detected with an anti-Flag M2 antibody and detection of β-actin was used as a loading control. *B,* HOXC10-expressing 1811 and HeLa cells show increased invasion through Matrigel-coated transwells compared with matched control (*Neo*) cells. *Columns,* mean of cells counted in five fields in each of three independent experiments; *bars,* SD. *C,* ectopic expression of HOXC10 in HeLa cells enhances anchorage-independent growth in soft agar. *Columns,* mean of colony number and size from three independent experiments; *bars,* SD.

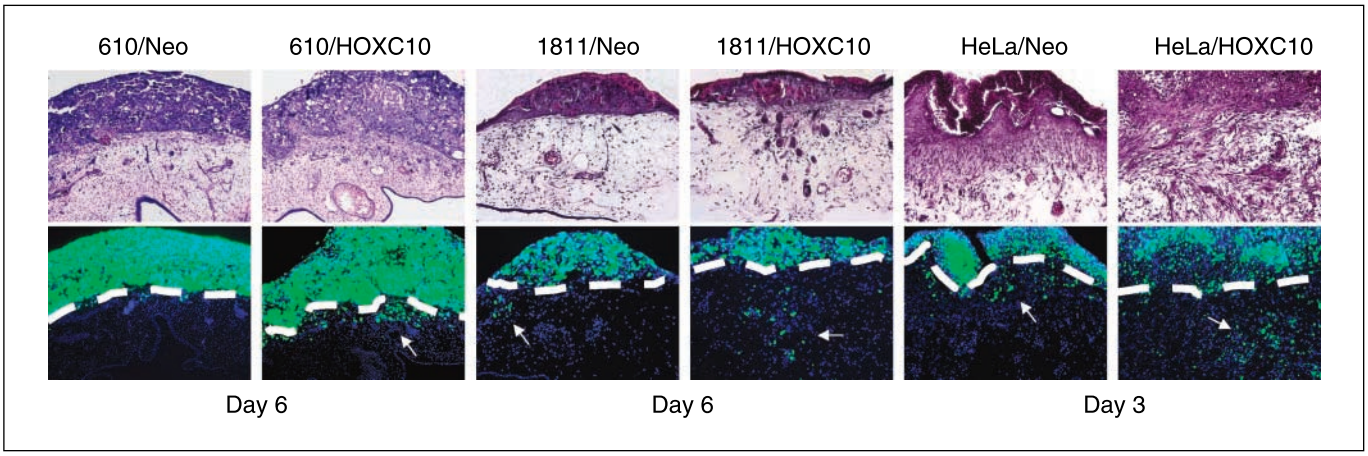

Figure 5. HOXC10 overexpression enhances invasion of 610, 1811, and HeLa cells in the chick CAM. *Top row,* the indicated cell lines were implanted on the CAM surface and at the indicated time points, CAM tissues were harvested, fixed, and stained with H&E. *Bottom row,* the same CAM tissues shown in the top row were also visualized by fluorescence because the implanted cells were labeled with Fluoresbrite carboxylated polystyrene nanospheres. The CAM surface is demarcated by dashed white lines. *Arrowheads,* cells invading the CAM.

between HSILs with high versus low risk for progression to invasive cancer would have significant clinical impact. Comparison of gene expression in HSILs and invasive cervical carcinomas allowed us to identify genes that may play important roles in, and/or serve as useful biomarkers for, this critical step in cervical cancer progression.

Our comparison of gene expression in invasive cervical carcinomas and their high-grade intraepithelial precursors identified a modest number of genes differentially up-regulated or down-regulated in SCCs versus HSILs. This is not necessarily surprising, given that HSILs and invasive carcinomas share many morphologic and molecular characteristics. Like invasive cervical carcinomas, HSILs are clonal, frequently aneuploid, and often harbor integrated HPV DNA (9, 29–32). One recent study that used DNA microarray data to identify chromosomal copy number alterations in preinvasive and invasive cervical carcinomas showed gains of chromosomes 12q and losses of 12p in both types of lesions (33). Moreover, in another comparison of gene expression in HSILs (specifically cervical intraepithelial neoplasia 3 or CIN3) and invasive cervical carcinomas using cDNA array filters allowing analysis of 1,176 "cancer-related" genes, fewer than 100 genes showed >2-fold up-regulation in invasive carcinomas compared with HSILs (28). These findings, as well as the results of our analysis, are in keeping with the notion that the neoplastic cells comprising HSILs share many biological properties with their frankly malignant counterparts, but lack the capacity to invade basement membrane and underlying cervical stroma.

The genes we found up-regulated in invasive SCCs relative to HSILs include several others previously described as overexpressed

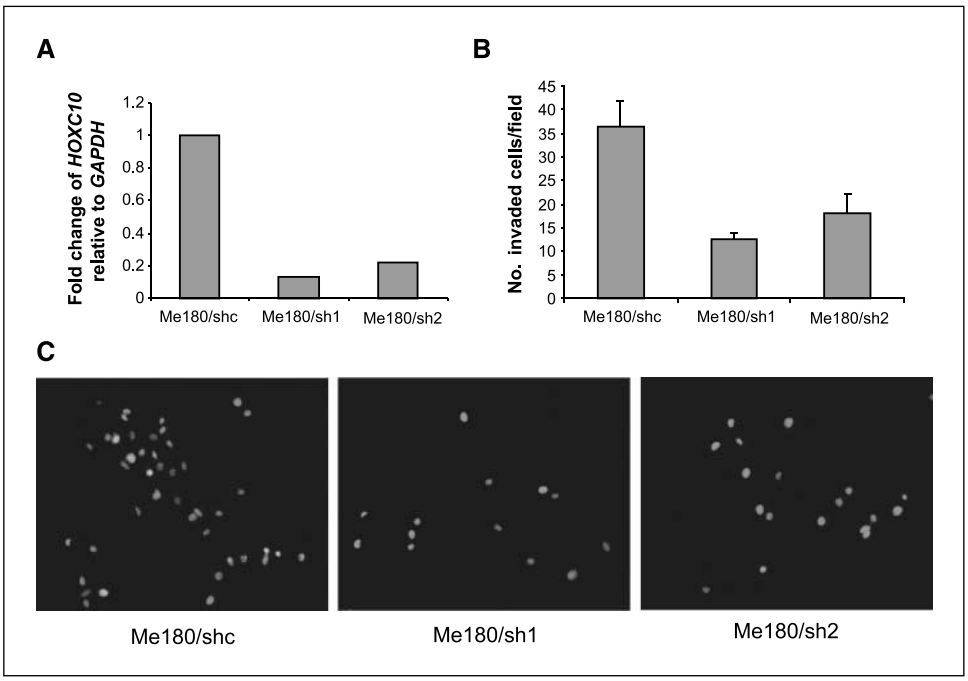

Figure 6. shRNA-mediated knockdown of *HOXC10* expression inhibits invasion of ME180 cells. *A, HOXC10* expression relative to *GAPDH* was analyzed by qRT-PCR in ME180 cells expressing two independent shRNAs (*sh1* and *sh2*) and one scrambled control shRNA (*shc*). *B,* ME180 cells with shRNA-mediated knockdown of *HOXC10* expression (*ME180/sh1* and *ME180/sh2*) show decreased invasion through Matrigel-coated transwells compared with matched control (*ME180/shc*) cells. *Columns,* mean of cells counted in five fields in each of three independent experiments; *bars,* SD. *C,* representative photomicrographs of ME180/shc, ME180/sh1, and ME180/sh2 cells penetrating the membrane.

in cervical cancers. These include *MCM2, PLOD2, ECT2, RFC4*, and *CDKN2A* (p16; refs. 25, 34–37). The proteins encoded by two of these, *MCM2* and *CDKN2A* (p16), have been used as markers for diagnosis of cervical neoplasia (36, 38, 39). *PLOD2, ECT2*, and *RFC4* reside on the long arm of chromosome 3 (3q23-24, 3q26, and 3q27 respectively). Notably, 10 of the 29 genes we found to be at least 2.5-fold overexpressed in SCCs relative to HSILs and normal cervical epithelia are on chromosome 3q (Fig. 1). A number of previous reports have described frequent gains or amplification of 3q in cervical carcinomas (33, 35, 40–42) and this molecular alteration often accompanies the progression from HSIL to invasive carcinoma (6). Additional studies will be required to distinguish those 3q genes with functional roles in cervical cancer progression from "bystander" genes that are overexpressed simply as a result of their proximity to genes whose increased copy number benefits the overall survival of tumor cells.

Interestingly, we showed that several homeobox genes (i.e., *HOXC10, HOXC6*, and *HOXD3*) are overexpressed in SCCs compared with HSILs. At least one of these, *HOXC10*, appears to be functionally associated with progression of HSIL to invasive carcinoma. Homeobox (Hox) transcription factors serve as important regulators of morphogenesis and differentiation during normal embryonic development (43, 44). Several Hox proteins, especially those in paralogue groups 9 to 13, function during female reproductive tract development (45). *HOX* genes also show characteristic patterns of expression in some normal adult organs, suggesting their possible roles in maintenance of tissue architecture. Several recent studies have suggested that dysregulation of specific homeobox genes is involved in cancer development, invasion, and metastasis, and altered expression patterns of homeobox genes have been observed in several different tumor types, including cancers of the lung, prostate, ovary, breast, colorectum, and cervix (reviewed by Abate-Shen in ref. 46). Selected Hox proteins have been shown to directly and indirectly regulate the expression of many angiogenic and growth factors, including basic fibroblast growth factor, vascular endothelial growth factor, interleukin-8, and Ang2 (47). Although promotion of angiogenesis by certain *HOX* genes may be essential for tumor invasion and metastasis, the overall pattern of homeobox gene expression, rather than expression of any one homeobox gene in a given cancer may be most important, given the functional redundancies of various Hox proteins (48).

Hung and colleagues (49) reported on RT-PCR analysis of 39 *HOX* genes in human cervical cancer–derived cell lines and found that *HOXC10* is expressed in cervical carcinoma cell lines but not in normal cervical tissues. They proposed that *HOXC10* (as well as *HOXA1, HOXB2, HOXB4, HOXC5*, and *HOXD13*) might be involved in cervical squamous epithelial transformation. More recently, Santin and colleagues (22) used oligonucleotide microarrays to compare gene expression in cervical carcinomas with normal keratinocytes, and found increased expression of both *HOXC6* and *HOXC10* in the cancer specimens relative to nonneoplastic keratinocytes. Hence, at least two other studies besides ours have implicated *HOXC10* in cervical cancer progression. However, our study would seem to be the first to show increased expression of *HOXC10* in invasive cancers relative to HSILs and to show that *HOXC10* enhances the motility, invasiveness, and anchorage-independent growth properties of squamous epithelial cells. Future studies should shed light on the molecular mechanisms by which *HOXC10* enhances cervical epithelial cell motility and invasiveness and whether the other up-regulated homeobox genes we identified (*HOXC6* and *HOXD3*) might have similar effects on cervical epithelial cells.

Acknowledgments

Received 6/4/2007; revised 8/10/2007; accepted 8/23/2007.

Grant support: National Cancer Institute Specialized Programs of Research Excellence in Cervical Cancer grant P50 CA098252 and the University of Michigan Comprehensive Cancer Center's Tissue Procurement Core facility grant 2P30 CA046592.

The costs of publication of this article were defrayed in part by the payment of page charges. This article must therefore be hereby marked *advertisement* in accordance with 18 U.S.C. Section 1734 solely to indicate this fact.

We thank F. Xavier Bosch (Servei d'Epidemiologia i Registre del Càncer, Institut Català d'Oncologia, Barcelona, Spain) and Nubia Muñoz (International Agency for Research on Cancer, Lyon, France) for providing cervical carcinoma samples for analysis, and Guido Bommer for helpful discussions.

References

1. Stat bite: Cervical cancer mortality worldwide. J Natl Cancer Inst 2006;98:434.
2. Wright TC, Jr., Kurman RJ, Ferenczy A, Kurman RJ. Precancerous lesions of the cervix. Blaustein's pathology of the female genital tract. 5th ed. New York: Springer-Verlag; 2002. p. 253–324.
3. Östör AG. Natural history of cervical intraepithelial neoplasia—a critical review. Int J Gynecol Pathol 1993; 12:186–92.
4. Trimble CL, Piantadosi S, Gravitt P, et al. Spontaneous regression of high-grade cervical dysplasia: effects of human papillomavirus type and HLA phenotype. Clin Cancer Res 2005;11:4717–23.
5. Walboomers JM, Jacobs MV, Manos MM, et al. Human papillomavirus is a necessary cause of invasive cervical cancer worldwide. J Pathol 1999;189:12–9.
6. Heselmeyer K, Schrock E, Dumanoir S, et al. Gain of chromosome 3q defines the transition from severe dysplasia to invasive carcinoma of the uterine cervix. Proc Natl Acad Sci U S A 1996;93:479–84.
7. Wistuba II, Montellano FD, Milchgrub S, et al. Deletions of chromosome 3p are frequent and early events in the pathogenesis of uterine cervical cancer. Cancer Res 1997;57:3154–8.
8. Duensing S, Munger K. Mechanisms of genomic instability in human cancer: insights from studies with human papillomavirus oncoproteins. Int J Cancer 2004; 109:157–62.
9. Park TW, Richart RM, Sun X-W, Wright TC, Jr. Association between human papillomavirus type and clonal status of cervical squamous intraepithelial lesions. J Natl Cancer Inst 1996;88:355–8.
10. Olaharski AJ, Sotelo R, Solorza-Luna G, et al. Tetraploidy and chromosomal instability are early events during cervical carcinogenesis. Carcinogenesis 2006;27:337–43.
11. Kaur P, McDougall JK. HPV-18 immortalization of human keratinocytes. Virology 1989;173:302–10.
12. De Geest K, Bergman CA, Turyk ME, et al. Differential response of cervical intraepithelial and cervical carcinoma cell lines to transforming growth factor-β1. Gynecol Oncol 1994;55:376–85.
13. Bosch FX, Muñoz N, de Sanjose S, et al. Risk factors for cervical cancer in Colombia and Spain. Int J Cancer 1992;52:750–8.
14. Yoshikawa H, Kawana T, Kitagawa K, et al. Detection and typing of multiple genital human papillomaviruses by DNA amplification with consensus primers. Jpn J Cancer Res 1991;82:524–31.
15. de Roda Husman AM, Walboomers JM, van den Brule AJ, et al. The use of general primers GP5 and GP6 elongated at their 3′ ends with adjacent highly conserved sequences improves human papillomavirus detection by PCR. J Gen Virol 1995;76:1057–62.
16. Gheit T, Landi S, Gemignani F, et al. Development of a sensitive and specific assay combining multiplex PCR and DNA microarray primer extension to detect high-risk mucosal human papillomavirus types. J Clin Microbiol 2006;44:2025–31.
17. Giordano TJ, Shedden KA, Schwartz DR, et al. Organ-specific molecular classification of primary lung, colon, and ovarian adenocarcinomas using gene expression profiles. Am J Pathol 2001;159:1231–8.
18. Zhai Y, Hotary KB, Nan B, et al. Expression of membrane type 1 matrix metalloproteinase is associated with cervical carcinoma progression and invasion. Cancer Res 2005;65:6543–50.
19. Rubinson DA, Dillon CP, Kwiatkowski AV, et al. A lentivirus-based system to functionally silence genes in primary mammalian cells, stem cells and transgenic mice by RNA interference. Nat Genet 2003;33: 401–6.
20. Kunzi-Rapp K, Genze F, Kufer R, et al. Chorioallantoic membrane assay: vascularized 3-dimensional cell culture system for human prostate cancer cells as an animal substitute model. J Urol 2001;166:1502–7.
21. Ossowski L. *In vivo* invasion of modified chorioallantoic membrane by tumor cells: the role of cell surface-bound urokinase. J Cell Biol 1988;107:2437–45.

22. Santin AD, Zhan F, Bignotti E, et al. Gene expression profiles of primary HPV16- and HPV18-infected early stage cervical cancers and normal cervical epithelium: identification of novel candidate molecular markers for cervical cancer diagnosis and therapy. Virology 2005; 331:269–91.
23. Bachtiary B, Boutros PC, Pintilie M, et al. Gene expression profiling in cervical cancer: an exploration of intratumor heterogeneity. Clin Cancer Res 2006;12: 5632–40.
24. Grigsby PW, Watson M, Powell MA, et al. Gene expression patterns in advanced human cervical cancer. Int J Gynecol Cancer 2006;16:562–7.
25. Wong YF, Cheung TH, Tsao GS, et al. Genome-wide gene expression profiling of cervical cancer in Hong Kong women by oligonucleotide microarray. Int J Cancer 2006;118:2461–9.
26. Chao A, Wang TH, Lee YS, et al. Molecular characterization of adenocarcinoma and squamous carcinoma of the uterine cervix using microarray analysis of gene expression. Int J Cancer 2006;119:91–8.
27. Chen Y, Miller C, Mosher R, et al. Identification of cervical cancer markers by cDNA and tissue microarrays. Cancer Res 2003;63:1927–35.
28. Sopov I, Sorensen T, Magbagbeolu M, et al. Detection of cancer-related gene expression profiles in severe cervical neoplasia. Int J Cancer 2004;112:33–43.
29. Enomoto T, Haba T, Fujita M, et al. Clonal analysis of high-grade squamous intra-epithelial lesions of the uterine cervix. Int J Cancer 1997;73:339–44.
30. Grote HJ, Nguyen HV, Leick AG, Bocking A. Identification of progressive cervical epithelial cell abnormalities using DNA image cytometry. Cancer 2004;102:373–9.
31. Cullen AP, Reid R, Champion M, Lorincz AT. Analysis of the physical state of different human papillomavirus DNAs in intraepithelial and invasive cervical neoplasia. J Virol 1991;65:606–12.
32. Hopman AH, Theelen W, Hommelberg PP, et al. Genomic integration of oncogenic HPV and gain of the human telomerase gene TERC at 3q26 are strongly associated events in the progression of uterine cervical dysplasia to invasive cancer. J Pathol 2006;210:412–9.
33. Fitzpatrick MA, Funk MC, Gius D, et al. Identification of chromosomal alterations important in the development of cervical intraepithelial neoplasia and invasive carcinoma using alignment of DNA microarray data. Gynecol Oncol 2006;103:458–62.
34. Ishimi Y, Okayasu I, Kato C, et al. Enhanced expression of Mcm proteins in cancer cells derived from uterine cervix. Eur J Biochem 2003;270:1089–101.
35. Narayan G, Bourdon V, Chaganti S, et al. Gene dosage alterations revealed by cDNA microarray analysis in cervical cancer: identification of candidate amplified and overexpressed genes. Genes Chromosomes Cancer 2007;46:373–84.
36. Agoff SN, Lin P, Morihara J, et al. p16(INK4a) expression correlates with degree of cervical neoplasia: a comparison with Ki-67 expression and detection of high-risk HPV types. Mod Pathol 2003;16:665–73.
37. Sano T, Oyama T, Kashiwabara K, et al. Immunohistochemical overexpression of p16 protein associated with intact retinoblastoma protein expression in cervical cancer and cervical intraepithelial neoplasia. Pathol Int 1998;48:580–5.
38. Shroyer KR, Homer P, Heinz D, Singh M. Validation of a novel immunocytochemical assay for topoisomerase II-α and minichromosome maintenance protein 2 expression in cervical cytology. Cancer 2006; 108:324–30.
39. Volgareva G, Zavalishina L, Andreeva Y, et al. Protein p16 as a marker of dysplastic and neoplastic alterations in cervical epithelial cells. BMC Cancer 2004;4:58.
40. Sugita M, Tanaka N, Davidson S, et al. Molecular definition of a small amplification domain within 3q26 in tumors of cervix, ovary, and lung. Cancer Genet Cytogenet 2000;117:9–18.
41. Heselmeyer K, Macville M, Schrock E, et al. Advanced-stage cervical carcinomas are defined by a recurrent pattern of chromosomal aberrations revealing high genetic instability and a consistent gain of chromosome arm 3q. Genes Chromosomes Cancer 1997;19:233–40.
42. Kirchhoff M, Rose H, Petersen BL, et al. Comparative genomic hybridization reveals non-random chromosomal aberrations in early preinvasive cervical lesions. Cancer Genet Cytogenet 2001;129:47–51.
43. Gehring WJ. Exploring the homeobox. Gene 1993;135: 215–21.
44. Mark M, Rijli FM, Chambon P. Homeobox genes in embryogenesis and pathogenesis. Pediatr Res 1997;42: 421–9.
45. Du H, Taylor HS. Molecular regulation of mullerian development by Hox genes. Ann N Y Acad Sci 2004;1034: 152–65.
46. Abate-Shen C. Deregulated homeobox gene expression in cancer: cause or consequence? Nat Rev Cancer 2002;2:777–85.
47. Care A, Felicetti F, Meccia E, et al. HOXB7: a key factor for tumor-associated angiogenic switch. Cancer Res 2001;61:6532–9.
48. Gorski DH, Walsh K. Control of vascular cell differentiation by homeobox transcription factors. Trends Cardiovasc Med 2003;13:213–20.
49. Hung YC, Ueda M, Terai Y, et al. Homeobox gene expression and mutation in cervical carcinoma cells. Cancer Sci 2003;94:437–41.

Gene Expression Analysis of Preinvasive and Invasive Cervical Squamous Cell Carcinomas Identifies *HOXC10* as a Key Mediator of Invasion

Yali Zhai, Rork Kuick, Bin Nan, et al.

Cancer Res 2007;67:10163-10172.